JACS
JOURNAL OF THE AMERICAN CHEMICAL SOCIETY

COMMUNICATION

pubs.acs.org/JACS

Crystal Structure of the Zinc-Dependent MarR Family Transcriptional Regulator AdcR in the Zn(II)-Bound State

Alfredo J. Guerra, Charles E. Dann, III, and David P. Giedroc*

Department of Chemistry, Indiana University, Bloomington, Indiana 47405, United States

Supporting Information

ABSTRACT: *Streptococcus pneumoniae* adhesin competence regulator (AdcR), the first metal-dependent member of the multiple antibiotic resistance regulator (MarR) family of proteins, represses the transcription of a high-affinity zinc-specific uptake transporter, a group of surface antigen zinc-binding pneumococcal histidine triad proteins (PhtA, PhtB, PhtD, and PhtE), and an AdcA homologue (AdcAII). The 2.0 Å resolution structure of Zn(II)-bound AdcR reveals a highly helical two-fold-symmetric dimer with two distinct metal-binding sites per protomer. Zn(II) is tetrahedrally coordinated by E24, H42, H108, and H112 in what defines the primary sensing site in AdcR. Site 2 is a tetracoordinate site whose function is currently unknown. NMR methyl group perturbation experiments reveal that Zn(II) drives a global change in the structure of apo-AdcR that stabilizes a conformation that is compatible with DNA binding. This co-repression mechanism is unprecedented in MarR transcriptional regulators.

Zinc ranks 23rd in crustal abundance and, after iron, is the second most abundant transition metal in human plasma.[1,2] As with many transition metal ions, zinc plays an important role in numerous and diverse biological reactions either as a structural component of proteins or as a cofactor in enzyme-catalyzed reactions.[3] Due to its role as an essential nutrient, microorganisms have developed zinc-specific membrane-associated transporters to concentrate Zn(II) ions.[4] However, in *Streptococcus pneumoniae*, an excess of zinc has been shown to induce a manganese deficiency, thus disrupting intracellular metal homeostasis.[5] To avoid imbalances in metal availability, bacteria have developed highly refined regulatory machinery to maintain transition metal homeostasis.[6,7] In prokaryotes, this response is mediated by metal sensor proteins that harbor specific metal coordination complexes that negatively or positively influence DNA binding and transcriptional repression.[8] These specialized metal receptor proteins coordinately control a highly selective adaptive response by regulating the expression of genes that mediate intracellular metal concentration and bioavailability.

In *S. pneumoniae*, the Zn(II)-selective ABC transporter genes (*adcABC*) are regulated by the first metal-dependent member of the multiple antibiotic resistance regulator (MarR) family of transcriptional regulators, adhesin competence regulator (AdcR).[9,10] AdcR also controls the transcription of four pneumococcal histidine triad proteins responsible for surface adhesion (PhtA, PhtB, PhtD, and PhtE) as well as a Zn(II)-specific AdcA homologue, AdcAII, of unknown function.[11,12] AdcB and the Pht proteins are required for pneumococcal virulence.[11] In order to further our understanding of the mechanism by which AdcR regulates its gene targets, we determined the structure of Zn(II)-AdcR by X-ray crystallography.

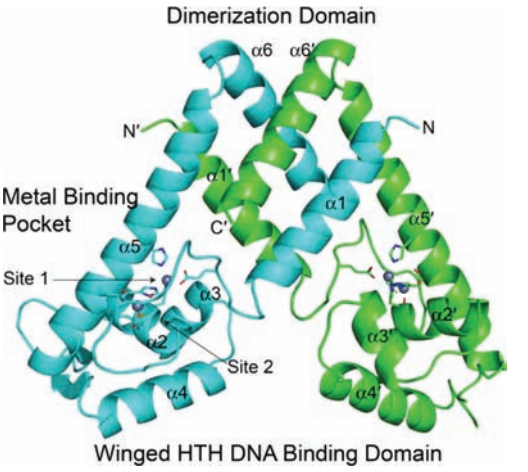

Figure 1. Ribbon representation of the 2.0 Å resolution crystal structure of dimeric Zn(II)-bound AdcR, with one protomer colored cyan and the other colored green. The two Zn(II) ions per protomer are represented by slate spheres, and coordinating ligands are shown as sticks. HTH = helix-turn-helix.

Zn(II)-AdcR crystallized in the orthorhombic space group $P2_12_12_1$ with one dimer per asymmetric unit. The structure was solved using single-wavelength anomalous dispersion on a Se-Met-substituted AdcR and refined to 2.0 Å resolution with an *R*-factor of 18.5% and a maximum-likelihood-based estimated coordinate error of 0.56 Å. The crystallographic data and refinement statistics are summarized in Table S1 of the Supporting Information. The Zn(II)-AdcR structure (Figure 1) resembles other structurally characterized MarR family proteins in that it is a triangularly shaped two-fold-pseudosymmetric homodimer. Both protomers are in similar conformations and superimpose with a root-mean-square deviation (rmsd) of 1.2 Å for the corresponding 129 Cα atoms (Figure S1). The most notable differences are localized in the helix-turn-helix (HTH) DNA-binding motif including the lack of density in one of the two β-wings. This is consistent with what has been observed in other DNA-free MarR structures.[13−15] Consistent with our previously published NMR data,[12] Zn(II)-AdcR is a highly α-helical protein

Received: August 25, 2011
Published: November 15, 2011

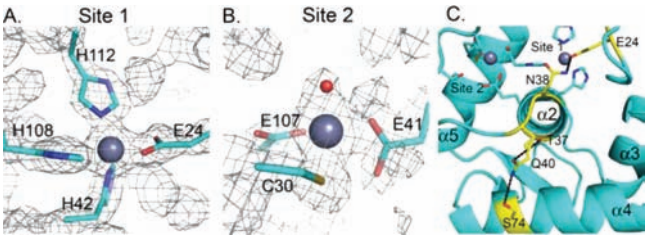

Figure 2. (A) Site 1 metal-binding residues (E24, H42, H108, and H112) with weighted $2mF_o - DF_c$ map contoured at 1.5σ. (B) Site 2 metal-binding residues (C30, E41, and E107) and coordinating water molecule with electron density contoured at 1.5σ. (C) Putative hydrogen-bonding network connecting site 1 to the DNA recognition helix, $\alpha 4$. Metal-coordinating side chains are represented as sticks, and hydrogen-bonding network residues are highlighted in yellow.

made up of six α-helices and a two stranded antiparallel β-hairpins as part of the winged helix motif. AdcR has two functional domains, a dimerization domain made up of the $\alpha 1$ helix, the C-terminal region of the $\alpha 5$ helix, and the $\alpha 6$ helix, and a winged HTH DNA-binding domain made up of $\alpha 2$, $\alpha 3$, $\alpha 4$, $\beta 1$, and $\beta 2$. The two domains are linked by the long $\alpha 5$ helix.

The dimerization domain connects to the DNA-binding domain via the $\alpha 2$ and $\alpha 5$ helices which, together with the extended $\alpha 1-\alpha 2$ loop, make up the metal-binding pocket. The metal-binding pocket reveals two distinct metal-binding sites shown in Figure 2. Zn(II) at site 1 (Figure 2A) is coordinated by the E24 Oε1, H42 Nδ1, H108 Nε2, and H112 Nε2 donor atoms in a distorted tetrahedral geometry. Mutant strains of *S. pneumoniae* harboring H108A and H112A substitutions are as sensitive to zinc toxicity as a Δ*adcR* deletion strain *in vivo*, while H42A, H108A, and H112A AdcR's fail to structurally switch upon Zn(II) binding and cannot be allosterically activated to bind the *adc* operator DNA *in vitro*.[12]

The site 2 Zn(II) ion (Figure 2B) is coordinated by three conserved side chains (C30, E41, and E107) and a water molecule arranged in a highly distorted tetrahedral geometry (Table S2). Inspection of the structure suggests some communication between the two metal-binding sites via a hydrogen bond between the non-liganding Nδ1 atom of H108 and the liganding Oε1 atom of E41 (Figure S2). Despite this, a C30A AdcR mis-sense strain exhibits wild-type-like zinc resistance, revealing that site 2 plays no significant role in this regulatory process.[12] Additionally, substitution of each glutamate in site 2 with alanine results in wild-type-like $^1H-^{15}N$ TROSY spectra for both the apo- and Zn(II)-bound forms (Figure S3). This reveals that site 1 is the primary sensing site in AdcR.

The observation of two bound Zn(II) per protomer, or four per dimer, however, is consistent with one pair of high-affinity site ($K_{Zn1} \approx 10^{12}$ M^{-1}, pH 8.0) and one pair of lower-affinity sites ($K_{Zn2} \approx 10^{7}$ M^{-1}, pH 8.0) per dimer as revealed by direct titration in solution.[12] The high-affinity sites correspond to site 1, since substitution of site 1 ligands decreases K_{Zn1} by $\geq$1000-fold with little effect on the affinity defined by K_{Zn2}. Interestingly, characterization of the high-affinity sites by X-ray absorption spectroscopy was more consistent with a pentacoordinate zinc coordinated by three histidine and two oxygen ligands rather than tetrahedral geometry observed in the crystal structure. Site 1 could easily adopt a trigonal bipyramidal structure with a relatively small movement of the E24 side chain to achieve bidentate coordination; such a displacement seems plausible, given that the non-liganding E24 Oε2, H42 Nε2, and H112 Nδ1 face of the chelate is fully exposed to solvent, with each atom hydrogen-bonded to a water molecule (Figure S4). This suggests that the metal-sensing site 1 of AdcR is structurally plastic, a feature paralleled by site 2 of the iron regulator Fur from *Helicobacter pylori*.[16]

Co(II) coordination by site 1 also reveals a coordination number of 5−6 rather than 4, and Co(II) allosterically activates DNA binding to an extent similar to that of Zn(II).[12] Paramagnetic NMR studies reveal that Co(II) binds to the metal-binding pocket defined by site 1 and induces a conformational change in the dimer that is very similar to that observed for Zn(II) binding (Figure S5). These titration data also suggest that a single monomer molar equivalent metal bound to site 1 is necessary and sufficient to change the global conformation of AdcR in solution. The biological selectivity of AdcR for zinc is dictated by metal affinity and bioavailability of Zn(II) versus Co(II), which is not expected to reach an intracellular concentration necessary to activate AdcR binding.

The two metal-binding sites sit on opposite sides atop the $\alpha 2$ helix in an arrangement that is reminiscent of the crystal structure of *Streptomyces coelicolor* Zur, a widespread bacterial zinc uptake regulator from the Fur family.[17] Interestingly, both *S. coelicolor* Zur and *S. pneumoniae* AdcR bind to multiple target promoters, thereby controlling the expression of multiple genes. *S. coelicolor* Zur has been postulated to use a secondary metal-binding site as a fine-tuning mechanism for activation of binding to a distinct set of target promoters.[17] Although our previous studies did not reveal a functional role for site 2 in global zinc resistance, further studies are required to determine if binding of Zn(II)-AdcR to its target promoters is modulated in some way by binding to site 2. It is interesting to note that the ligands coordinating to each metal site are absolutely conserved in AdcR's (Figure S6).

The metal-binding pocket of AdcR appears connected to the DNA recognition helix via a hydrogen-bonding network shown in Figure 2C. Here the liganding Oε1 atom from E24 accepts a hydrogen bond from the carboxamide side chain of N38. The $\alpha 2$ helix is then connected to the DNA recognition helix, $\alpha 4$, via a hydrogen bond between the side chains of Q40 and S74. This latter hydrogen bond is also found in the DNA-free and DNA-bound SlyA structures involving the Nε2 atom of H33 and the carbonyl oxygen of the carboxamide side chain of Q69.[13] The distance between these two atoms is 2.6 Å, which increases to 3.3 Å in the structure of *Salmonella typhimurium* SlyA complexed with an allosteric inhibitor salicylate (PDB code 3DEU). This suggests that the hydrogen-bonding network observed in the Zn(II)-AdcR structure (Figure 2C) may play an important role in the allosteric positive regulation of DNA binding by Zn(II) in AdcR's. Experiments are underway to pinpoint the origin of the ≤ -4.0 kcal mol^{-1} allosteric coupling free energy that links Zn(II) binding to DNA binding.[12]

While the overall fold of Zn(II)-AdcR is similar to that of other structurally characterized MarR family regulators, there are substantial differences, as illustrated by a comparison of Zn(II)-AdcR and ligand-free SlyA (Figure 3). AdcR has a shorter $\alpha 1$ helix (residues 3−19), leading to a subsequent lengthening of the $\alpha 1-\alpha 2$ loop (residues 20−37). This loop contains two conserved metal-binding residues among putative AdcR's, E24 and C30 (Figure S6). Furthermore, the N-terminal region of the $\alpha 5$ helix lacks a kink that is common in other structurally characterized MarR regulators. These two differences lead to the formation of a pocket that accommodates high-affinity zinc binding while

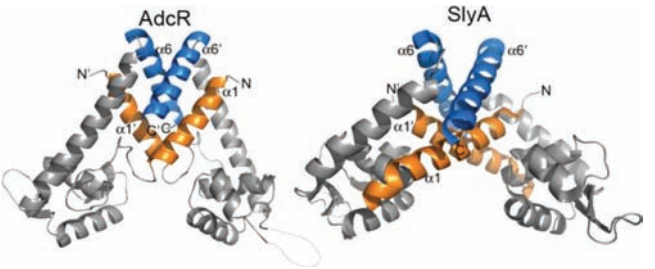

Figure 3. Comparison of the Zn(II)-AdcR structure to the SlyA dimer in the DNA-bound form. The DNA in the SlyA structure is not shown for clarity, and the α1 and α6 helices are highlighted in orange and blue, respectively.

maintaining plasticity to adopt different coordination numbers. Additionally, the relative orientation of the α1 and α6′ helices is virtually parallel in the Zn(II)-AdcR structure, as opposed to the more perpendicular orientation that is observed in other MarR structures (Figure 3).[14,18] These structural differences account for the high rmsd (5.8 Å for 105 corresponding Cα atoms) in the superimposition of the DNA-bound SlyA dimer onto the Zn(II)-AdcR dimer. However, as observed with other MarR family members, the superimposition of the HTH motif of the DNA-bound SlyA and Zn(II)-AdcR reveals a high degree of similarity, with rmsd = 0.50 Å for 19 corresponding Cα atoms (Figure S7).[19]

Previous structures of DNA-free and ligand-free MarR family proteins reveal conformations that are incompatible with high-affinity DNA binding, and thus likely bind to the DNA via induced fit. For example, the drug-free MepR structure adopts a very "open" conformation, with the two recognition helices ~43 Å apart.[19] Additionally, the apo-SlyA structure has been shown to be in a "closed" position, with the recognition helices ~15 Å apart, also incompatible with the distance between successive major grooves in B-form DNA (34 Å).[13] In the Zn(II)-AdcR structure, the two recognition helices (α4 and α4′) are oriented in an open conformation, separated by ~30 Å, clearly poised for DNA binding. This is consistent with the distances measured between the recognition helices of *Bacillus subtilis* OhrR bound to DNA (31 Å)[18] and *Salmonella enterica* SlyA bound to DNA (32 Å).[13] Presumably, binding of DNA to Zn(II)-AdcR would remodel the DNA-binding interface slightly so that the reading heads fit into consecutive major grooves while twisting the wing to allow for contacts with the flanking minor grooves. This remodeling might also allow for the N-terminal region of the α1−α2 loop to dip into the interior minor groove and make contacts with the DNA.

Our previous NMR studies have shown that there are large global perturbations in the ^{1}H−^{15}N TROSY spectrum of AdcR upon the addition of Zn(II) to apo-AdcR (Figure S5B, right). This is consistent with a structural switch that stabilizes a high-affinity DNA-binding conformation, although the magnitude of this structural change is not yet known.[12] Additionally, it is interesting to note that residues 21−26 and 37−40 in the α1−α2 loop are conformationally exchange-broadened in the absence of bound Zn(II), and this effect is quenched upon metal binding to AdcR. Further evidence in support of this conformational switch comes from examination of the methyl group chemical shift perturbation maps, where the changes in chemical shift of all assigned methyl groups for the Zn(II)-bound and DNA-bound Zn(II)-AdcR relative to the weakly binding apo-AdcR and Zn(II)-AdcR reference states, respectively, are shown

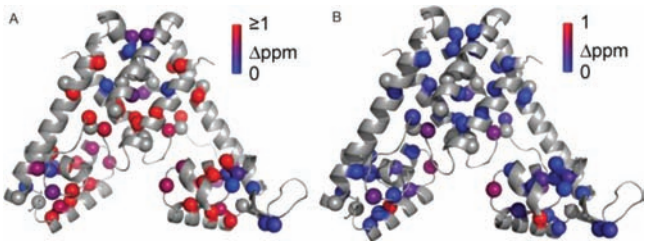

Figure 4. Methyl group perturbation upon (A) Zn(II) binding to apo-AdcR (0.01−2.62 ppm) and (B) DNA binding by Zn(II)-AdcR (0.012−0.94 ppm). Chemical shift perturbations were calculated using $\Delta\delta = [(\Delta\text{ppm }^{1}\text{H})^2 + (\Delta\text{ppm }^{13}\text{C}/4)^2]^{1/2}$.

(Figure 4). As can be seen, the chemical shift perturbations are large in magnitude and distributed throughout the entire dimeric molecule when comparing the apo and Zn(II) states, from the regulatory sites, to the DNA-binding domain and the region that connects the two domains (Figure 4A). In contrast, on moving from the Zn(II) bound state to the repressing ternary complex, the chemical shift changes are smaller in magnitude, with the larger perturbations localized to what is anticipated to be much of the protein−DNA interface (Figure 4B). These data are fully consistent with a significant change in the quaternary structure driven by Zn(II) allosteric activation.

With few exceptions, effector molecules interact with MarR homologues, resulting in a low DNA affinity state. These effector ligands either directly bind to the protein or lead to a covalent modification, specifically cysteine oxidation. For example, *Deinococcus radiodurans* HucR binds to its promoter DNA in the apo form, and the affinity is greatly reduced in the presence of the inducer uric acid.[20] Similarly, the *marRAB* operator DNA-binding affinity of the founding member of this protein family, *Escherichia coli* MarR, is reduced in the presence of salicylate, plumbagin, and menadione, among other inducers.[21] Salicylate has also been shown to disrupt the SlyA-DNA complex in a gel shift assay.[13] Likewise, both salicylate and benzaldehyde have been shown to act as de-repressors in the archaeal MarR homologue BldR2.[22]

In a second class of MarR homologues, the repressor reacts with oxidizing agents that modify regulatory cysteine residues, leading to de-repression of target genes. *B. subtilis* OhrR represses the transcription of an organic peroxide resistance gene *ohrA*. Oxidation of the lone cysteine residue in OhrR to sulfenic acid by organic hydrogenperoxides leads to OhrR dissociation from the DNA, thus allowing for transcription of the *ohrA* gene.[23] In a slightly different mechanism, *Xanthomonas campestris* OhrR uses a cysteine pair to form an interprotomer disulfide bond that results in de-repression of DNA. For the archaeal MarR homologue BldR, ligand-mediated activation of DNA binding leads to transcription activation.[24] These observations illustrate the wide diversity of possible allosteric mechanisms and transcriptional regulation in the MarR family of proteins.

AdcR differs from the previously described members of the MarR family in two important ways. First, AdcR (ZitR in *Lactococcus lactis*[25]) has a unique effector in Zn(II). Additionally, the co-repression mechanism induced by metal binding to AdcR is unprecedented in MarR family transcriptional regulators. The Zn(II)-AdcR structure presented here provides the first structural glimpses of the mechanism of transcription co-repression in the MarR family, as well as a starting point for understanding allosteric activation by zinc in AdcR in detail.

■ ASSOCIATED CONTENT

Supporting Information. Supplementary table and experimental procedures. This material is available free of charge via the Internet at http://pubs.acs.org. The atomic coordinates and structure factors have been deposited in the Protein Data Bank as entry 3TGN.

■ AUTHOR INFORMATION

Corresponding Author
giedroc@indiana.edu

■ ACKNOWLEDGMENT

We thank Dr. Jay Nix and the staff of Beamline 4.2.2 of the Advanced Light Source for help in data collection. The ALS is supported by the Director, Office of Science, Office of Basic Energy Sciences, Materials Sciences Division, of the U.S. Department of Energy under Contract No. DE-AC03-76SF00098 at Lawrence Berkeley National Laboratory. We also thank Dr. Xiangming Kong at Texas A&M University and Dr. Dejian Ma at Indiana University for their help with NMR experimental setup. This work was supported by a grant from the NIH (GM042569).

■ REFERENCES

(1) Shriver, D. F.; Atkins, P. W. *Inorganic Chemistry*, 3rd ed.; Oxford University Press: Oxford, 1999.
(2) Theil, E. C.; Raymond, K. N. In *Bioinorganic chemistry*; Bertini, I., Gray, H. B., Lippard, S. J., Valentine, J. S., Eds.; University Science Books: Mill Valley, CA, 1994; p viii.
(3) Fraústo da Silva, J.; Williams, R. *The Biological Chemistry of Elements: The Inorganic Chemistry of Life*, 2nd ed.; Oxford University Press: Oxford, 2001.
(4) Ma, Z.; Jacobsen, F. E.; Giedroc, D. P. *Chem. Rev.* **2009**, *109*, 4644.
(5) Jacobsen, F. E.; Kazmierczak, K. M.; Lisher, J. P.; Winkler, M. E.; Giedroc, D. P. *Metallomics* **2011**, *3*, 38.
(6) Tottey, S.; Harvie, D. R.; Robinson, N. J. *Acc. Chem. Res.* **2005**, *38*, 775.
(7) O'Halloran, T. V. *Science* **1993**, *261*, 715.
(8) Giedroc, D. P.; Arunkumar, A. I. *Dalton Trans.* **2007**, *29*, 3107.
(9) Panina, E. M.; Mironov, A. A.; Gelfand, M. S. *Proc. Natl. Acad. Sci. U.S.A.* **2003**, *100*, 9912.
(10) Claverys, J. P. *Res. Microbiol.* **2001**, *152*, 231.
(11) Ogunniyi, A. D.; Grabowicz, M.; Mahdi, L. K.; Cook, J.; Gordon, D. L.; Sadlon, T. A.; Paton, J. C. *FASEB J.* **2009**, *23*, 731.
(12) Reyes-Caballero, H.; Guerra, A. J.; Jacobsen, F. E.; Kazmierczak, K. M.; Cowart, D.; Koppolu, U. M.; Scott, R. A.; Winkler, M. E.; Giedroc, D. P. *J. Mol. Biol.* **2010**, *403*, 197.
(13) Dolan, K. T.; Duguid, E. M.; He, C. *J. Biol. Chem.* **2011**, *286*, 22178.
(14) Newberry, K. J.; Fuangthong, M.; Panmanee, W.; Mongkolsuk, S.; Brennan, R. G. *Mol. Cell* **2007**, *28*, 652.
(15) Poor, C. B.; Chen, P. R.; Duguid, E.; Rice, P. A.; He, C. *J. Biol. Chem.* **2009**, *284*, 23517.
(16) Dian, C.; Vitale, S.; Leonard, G. A.; Bahlawane, C.; Fauquant, C.; Leduc, D.; Muller, C.; de Reuse, H.; Michaud-Soret, I.; Terradot, L. *Mol. Microbiol.* **2011**, *79*, 1260.
(17) Shin, J.-H.; Jung, H. J.; An, Y. J.; Cho, Y.-B.; Cha, S.-S.; Roe, J.-H. *Proc. Natl. Acad. Sci. U.S.A.* **2011**, *108*, 5045.
(18) Hong, M.; Fuangthong, M.; Helmann, J. D.; Brennan, R. G. *Mol. Cell* **2005**, *20*, 131.
(19) Kumaraswami, M.; Schuman, J. T.; Seo, S. M.; Kaatz, G. W.; Brennan, R. G. *Nucleic Acids Res.* **2009**, *37*, 1211.
(20) Wilkinson, S. P.; Grove, A. *J. Biol. Chem.* **2004**, *279*, 51442.
(21) Alekshun, M. N.; Levy, S. B. *J. Bacteriol.* **1999**, *181*, 4669.
(22) Fiorentino, G.; Del Giudice, I.; Bartolucci, S.; Durante, L.; Martino, L.; Del Vecchio, P. *Biochemistry* **2011**, *50*, 6607.
(23) Fuangthong, M.; Helmann, J. D. *Proc. Natl. Acad. Sci. U.S.A.* **2002**, *99*, 6690.
(24) Fiorentino, G.; Ronca, R.; Cannio, R.; Rossi, M.; Bartolucci, S. *J. Bacteriol.* **2007**, *189*, 7351.
(25) Llull, D.; Son, O.; Blanie, S.; Briffotaux, J.; Morello, E.; Rogniaux, H.; Danot, O.; Poquet, I. *J. Bacteriol.* **2011**, *193*, 1919.

■ NOTE ADDED IN PROOF

A paper that appeared during the review of this manuscript establishes that AdcA and AdcAII perform redundant functions in zinc uptake in *Streptococcus pneumoniae* (Bayle, L.; Chimalapati, S.; Schoehn, G.; Brown, J.; Vernet, T.; Durmort, C. *Mol. Microbiol.* **2011**, *82*, 904.